Anomalous and normal diffusion of proteins and lipids in crowded lipid membranes

Matti Javanainen,[a] Henrik Hammaren,[a] Luca Monticelli,[b] Jae-Hyung Jeon,[a] Markus S. Miettinen,[c] Hector Martinez-Seara,[a] Ralf Metzler[ad] and Ilpo Vattulainen*[ae]

Received 27th April 2012, Accepted 1st June 2012
DOI: 10.1039/c2fd20085f

Lateral diffusion plays a crucial role in numerous processes that take place in cell membranes, yet it is quite poorly understood in native membranes characterized by, *e.g.*, domain formation and large concentration of proteins. In this article, we use atomistic and coarse-grained simulations to consider how packing of membranes and crowding with proteins affect the lateral dynamics of lipids and membrane proteins. We find that both packing and protein crowding have a profound effect on lateral diffusion, slowing it down. Anomalous diffusion is observed to be an inherent property in both protein-free and protein-rich membranes, and the time scales of anomalous diffusion and the exponent associated with anomalous diffusion are found to strongly depend on packing and crowding. Crowding with proteins also has a striking effect on the decay rate of dynamical correlations associated with lateral single-particle motion, as the transition from anomalous to normal diffusion is found to take place at macroscopic time scales: while in protein-poor conditions normal diffusion is typically observed in hundreds of nanoseconds, in protein-rich conditions the onset of normal diffusion is tens of microseconds, and in the most crowded systems as large as milliseconds. The computational challenge which results from these time scales is not easy to deal with, not even in coarse-grained simulations. We also briefly discuss the physical limits of protein motion. Our results suggest that protein concentration is anything but constant in the plane of cell membranes. Instead, it is strongly dependent on proteins' preference for aggregation.

1 Introduction

Lateral diffusion of lipids and proteins[1,2] is one of the most significant dynamic processes in cell membranes, as it governs a variety of phenomena such as formation of membrane protein complexes and self-assembly of functional nano-scale membrane domains known as lipid rafts.[3] Understanding how these complex processes take place in native cell membranes under biologically relevant conditions

[a]*Department of Physics, Tampere University of Technology, P.O. Box 692, FI–33101 Tampere, Finland. E-mail: ilpo.vattulainen@tut.fi*
[b]*INSERM, UMR-S665, DSIMB 75015, Université Paris Diderot - Paris 7, UFR Life Sciences, Paris, France*
[c]*Fachbereich Physik, Freie Universität Berlin, 14195 Berlin, Germany*
[d]*Institute for Physics & Astronomy, University of Potsdam, Karl-Liebknecht-Strasse 24/25, D-14476 Potsdam-Golm, Germany*
[e]*MEMPHYS Center for Biomembrane Physics, University of Southern Denmark, Odense, Denmark*

is key to unlocking many of the cellular functions. In this work, we focus on one of the central issues in this context, that is, the effects of lipid packing and protein crowding on lipid and protein diffusion.

In cell membranes, their local surface density depends quite substantially on lipid composition. Membrane regions rich in polyunsaturated lipids are loosely packed, while in cholesterol and sphingolipid rich regions the packing of lipids is much tighter.[4–6] Especially the latter situation is appealing since the concept of lipid rafts is largely based on the interplay of cholesterol and sphingolipids that are abundant in these highly ordered and packed domains. Considering the heterogeneity of cell membranes and the spatially varying membrane density in the membrane plane, there is reason to expect that lateral diffusion also depends on lipid packing. Experiments on model membranes support this view.[7,8]

Meanwhile, given that in native membranes the (molar) ratio of proteins and lipids has been suggested[9,10] to vary roughly between 1 : 50 and 1 : 100, it is obvious that membranes in living cells can be crowded with proteins.[11] What does this mean in practice? Assuming a typical phospholipid whose area per lipid is 0.64 nm^2 and an alpha-helical transmembrane peptide/protein whose diameter is 3 nm, then for a protein-to-lipid number ratio of 1 : 50, the average distance between the proteins' surfaces is about 3.2 nm. This suggests that in membranes crowded with proteins, membrane-mediated protein–protein interactions may play decisive roles in lateral diffusion.

Packing and crowding may also play a role in the nature of diffusion, since in other biological contexts, such as in the cytoplasm of living cells it has been found that diffusion of individual molecules at "short" time scales is anomalous[12,13] (also called subdiffusion), with the average mean-squared displacement scaling as a power-law t^{α} in time t with an anomalous scaling exponent $\alpha < 1$.[14] Similar behavior has been suggested very recently for membrane channels in plasma membranes of human kidney cells.[15] At long times, if molecular motion is not confined to a certain region, one expects a random walk-like normal diffusion with $\alpha = 1$.

While most of the discussion relates to normal diffusion occurring at long times and large length scales, the concept and the biological relevance of crowding-induced anomalous diffusion have recently received increased attention, opening up new vistas for interesting implications. In the cytoplasm of living cells anomalous diffusion of tracers such as labelled messenger RNA,[12] lipid granules,[13] or chromosomal loci[16] have been observed on time scales of tens of seconds, in accordance with control experiments in dense dextran[17] or protein solutions.[18] At longer times this anomalous motion is of the type of viscoelastic subdiffusion. As found by Golding and Cox[12] as well as Guigas and Weiss,[19] viscoelastic subdiffusion leads to increased recurrence of the position coordinate and may lead to increased local reaction rates of diffusing reactants. Anomalous diffusion may also lead to dynamical localisation, as argued for chromosomal separation in eukaryotes from measurements of the telomere motion,[20] with similar consequences for the membrane channels investigated in ref. 15. Finally, anomalous diffusion would strongly influence the dynamics of surface-bulk exchange.[21,22]

As far as membrane proteins and lipids are concerned, the current understanding of their lateral diffusion is almost completely based on considerations in rather idealized conditions compared to a real biological environment, as the issues due to, *e.g.*, crowding, have not been clarified. Nonetheless, recent progress has provided a great deal of new insight into the mechanisms and physical laws associated with lipid and protein motion under protein-poor conditions. For instance, atomistic simulations recently showed[23] that the so-called free-volume theories[24–26] often used to interpret lipid diffusion data are incomplete, as they do not account for the proper diffusion mechanism of lipids. Unlike assumed earlier, the mechanism by which lipids diffuse in the plane of a membrane turned out to be a concerted one, based on tens of lipids moving in unison as loosely defined dynamical clusters.[23,27] These predictions based on simulations were recently verified by quasi-elastic neutron scattering

experiments.[28] Also, it has been found that not only lipid diffusion but also protein motion is based on concerted effects, as atomistic as well as coarse-grained simulations have highlighted membrane proteins to diffuse as dynamical clusters together with about 100 lipids around them,[29] the size of the complex being much larger than the size of the protein itself. As the current paradigm of membrane protein diffusion in protein-poor membranes is based on the Saffman–Delbrück model,[30] which describes the protein diffusion coefficient in terms of physical parameters such as protein size, even the understanding of lateral diffusion in protein-poor conditions is an important goal.

However, when more complex situations have been considered, experiments have shown that in native cell membranes the diffusion of proteins and lipids can be distinctly different compared to simplified model systems.[31–36] One of the striking findings is that if identical proteins undergo lateral diffusion in the membranes of seemingly identical cells, the diffusion coefficients determined for individual proteins in different regions of a membrane may be quite different, differing by a factor of five.[33] This conclusion seems to hold true regardless of the fact that the motion of the proteins has been followed up to macroscopic time scales. Meanwhile, diffusion of lipids can also be quite complex. Recent super-resolution microscopy studies of living cells have shown that the motion of lipids can be slowed down significantly on time scales of the order of milliseconds and length scales of tens of nanometers,[34] suggesting that there are unknown mechanisms to confine diffusion of specific lipid types.

While these two examples are just suggestive, they highlight the complexity of molecular motion in membrane systems. There are many factors that can affect how rapidly molecules diffuse in membranes, and it is quite plausible that many of them contribute at the same time. First, the roles of the actin and cytoskeleton networks are often important, as they create domains that confine molecular motion.[35] Specific lipid–protein and protein–protein interactions can also contribute, slowing down diffusion through complex formation. Lipids in the vicinity of membrane proteins are known to diffuse much more slowly compared to lipids far from proteins.[29] Furthermore, it is clear that crowding can have an influence on lateral molecular motion, since with large enough protein concentrations the motion of lipids and proteins will be blocked.[32,37,38] Overall, one can conclude that the complexity of native cell membranes renders studies of protein and lipid diffusion quite difficult, and care is warranted when the results are being interpreted.

The main objective of this work is to shed light on the implications of crowding on the dynamics of lipids and membrane proteins. This broad topic embraces considerations of how lateral diffusion coefficients depend on crowding of proteins and molecular packing of lipids, and how the time scales of anomalous diffusion and its exponent relate to crowded conditions. For lipids, anomalous diffusion has been identified in previous studies,[39–41] but its biological significance has remained unclear. As for membrane proteins, recent simulations have identified anomalous diffusion to be an intrinsic property of protein motion under crowding,[38] though its biological relevance is not understood.

Here we have considered these topics from two complementary viewpoints. First, we have elucidated crowding in the sense of *packing* through atomistic simulations of protein-free lipid monolayers, with a purpose to understand how membrane density affects lipid dynamics in the membrane plane. In a biological context, this is a relevant question, *e.g.*, during the respiratory cycle during which the monolayer-like lung surfactant is first expanded and then compressed. Second, we investigated how *crowding of membrane proteins* affects lateral dynamics in tensionless lipid bilayers. This topic is biologically highly relevant since—as mentioned above—native cell membranes are rich in proteins.

We have found that anomalous diffusion is an inherent property in both protein-free and protein-rich membranes, and that the time scales of anomalous diffusion and the anomalous diffusion exponents of lipids and proteins strongly depend on

packing/crowding. Strikingly, while in protein-poor conditions normal diffusion is observed in hundreds of nanoseconds, in protein-rich (crowded) conditions the onset of normal diffusion takes place in tens of microseconds, and in the most crowded systems quite likely on time scales that are no less than milliseconds. Given that the time scales associated with normal diffusion are so long, this matter has to be accounted for in analysis of diffusion data, and especially in simulations where the time scale problem is very severe even with coarse-grained simulation models. Moving on, we also discuss physical limits of protein motion, paying attention to the optimal protein concentration where protein diffusion would be fast enough to enable sufficiently rapid motion over large length scales and also promote protein–protein collisions needed for protein complex formation.

2 Methodology

2.1 Langmuir monolayers

We used atomistic molecular dynamics (MD) simulations to consider seven Langmuir monolayer systems with a mean molecular area ranging from 44 Å^2 to 68 Å^2, with a uniform spacing of 4 Å^2. With this range of compression, the monolayer states cover liquid condensed to liquid expanded phases. Further compression was found to result in monolayer buckling, while further expansion induced formation of holes.

The studied systems consisted of two monolayers separated by a water slab and a thick vacuum region to separate the monolayers from one another (see Fig. 1 for snapshots of individual monolayers in the systems). The monolayers contained 100 lipid molecules each, with the composition of 60 mol% dipalmitoylphosphatidylcholine (DPPC), 20 mol% palmitoyloleoylphosphatidylcholine (POPC), 10 mol% palmitoyloleoylphosphatidylglycerol (POPG), and 10 mol% cholesterol, in

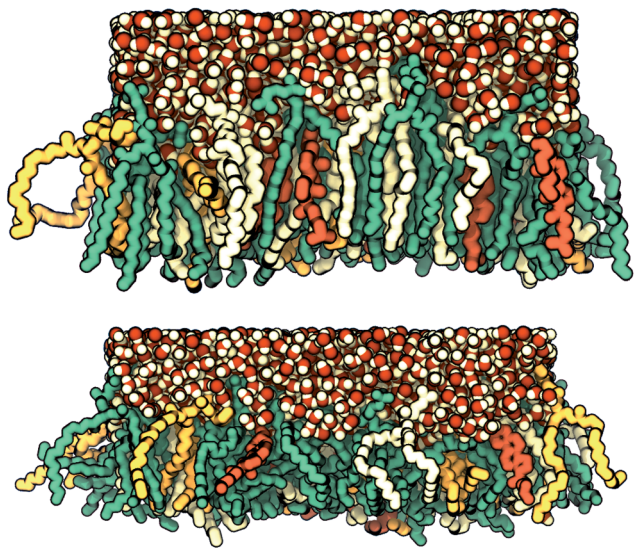

Fig. 1 Snapshots of the monolayer systems at a water–air interface at two different compressions: a fairly compressed system with $\langle A \rangle = 48$ Å^2 is shown above and a system with a lower surface pressure and $\langle A \rangle = 64$ Å^2 is depicted below. Lipids are drawn in the liquorice scheme with DPPC presented in green, POPC in white, POPG in yellow, and cholesterol in orange. Water is shown using the van der Waals scheme. For clarity, lipids on the sides have not been truncated but there are still periodic boundaries on both sides. Snapshots have been rendered with VMD.

agreement with experimental measurements on the human lung surfactant.[42] Extensive hydration was achieved with 7235 water molecules. A concentration of 150 mMol of NaCl was included in order to mimic physiological conditions. Additional sodium ions were added to neutralize the negative charges in POPG head groups. Two systems with mean molecular areas equal to 48 $Å^2$ and 64 $Å^2$ are represented in Fig. 1, showing clearly the difference in the ordering of their tails.

As described in our earlier work,[43] the force fields used for lipids followed the Berger description,[44] for cholesterol we used the description of Holtje *et al.*,[45] and for water we used the TIP3P model.[46] Salt and counterions were described by the GROMACS force field.

All simulations were conducted using the GROMACS simulation package.[47] The leap-frog integrator was employed in all simulations with a time step of 2 fs. NVT conditions were applied with temperature kept constant at 310 K with the Nosé–Hoover thermostat[48] with a time constant of 0.5 ps. Electrostatics were handled with the PME algorithm[49] of the order of 4. The cut-off used between real and inverse space calculations was 1 nm. The Lennard-Jones potential was cut-off at 1 nm and the neighbor list for the long-range interactions with a radius of 1 nm was updated every 10 steps. All bonds were constrained with LINCS[50] of the order of 4. Further details of the simulation model and protocol can be found from ref. 43.

Three sets of simulations were performed with different sampling frequencies in order to obtain information of lipid motion over a wide range of time scales from tens of femtoseconds to hundreds of nanoseconds. The shortest simulations were ran for 500 ps with data collected every 10 fs. The values for the second set were 10 ns and 100 fs, respectively. Finally, all the systems were simulated for at least 100 ns with coordinates saved every 10 ps. As the regime of normal diffusion was not achieved even after 100 ns, the simulations of the limiting cases of the most expanded and the most compressed systems were further extended to 660 ns and 610 ns, respectively. Data corresponding to the first 10% of the trajectories were discarded in all analyses.

2.2 Membrane proteins in lipid bilayers

To consider the joint lateral diffusion of proteins and lipids in membranes, we used coarse-grained (CG) models for two different one-component lipid bilayers to host membrane proteins. The first set of bilayers was composed of dilinoleoylphosphatidylcholine (DLPC) lipids, while the second one was comprised of dipalmitoylphosphatidylcholine (DPPC) lipids. These bilayers were simulated with a varying number of NaK channel (2AHY) proteins embedded in the membranes. The starting structures consisted of proteins positioned in a grid in the membrane plane.

The choice of these lipids and proteins was based on careful testing that concluded their properties to be distinctly different with respect to protein aggregation. In DLPC bilayers, NaK channels were found to avoid aggregation due to the minor hydrophobic mismatch between the proteins and the lipid bilayer. In DPPC bilayers, the situation was completely different, as NaK proteins were observed to prefer forming aggregates due to their larger hydrophobic mismatch. Therefore, the choice of lipids and proteins in our models is not based on their biological relevance but instead is just pragmatic: with these choices we can model two different scenarios, one preferring protein aggregation (DPPC) and another avoiding it (DLPC). In this spirit, the DPPC and DLPC systems are from here on referred to as aggregating (A) and non-aggregating (NA), respectively. Snapshots of chosen systems in the end of simulations are shown in Fig. 2.

Both systems were studied with multiple protein-to-lipid ratios (1 : 50, 1 : 75, 1 : 100, 1 : 150, and 1 : 200 in each leaflet, see Table 1) to consider diffusion at different levels of crowding. In addition, systems with a single protein embedded in a bilayer were also considered to describe dilute (protein-poor) conditions that we here denote as a protein-to-lipid ratio as 1 : infinity. The simulated systems

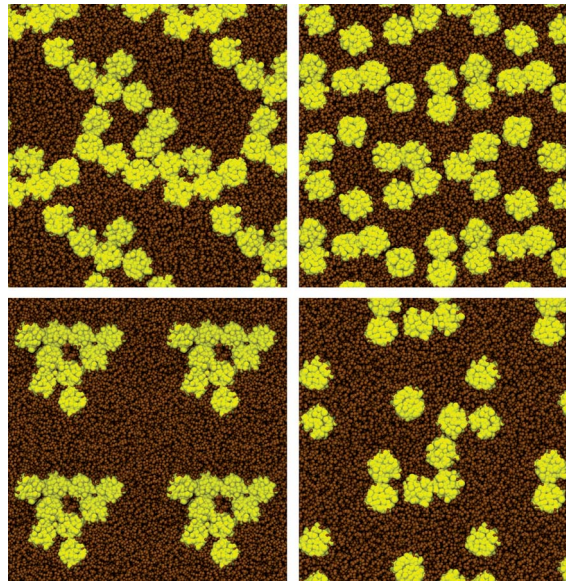

Fig. 2 Snapshots of protein–lipid systems with selected protein-to-lipid ratios. The aggregating DPPC system (A) is shown on the left hand side and the non-aggregating DLPC (NA) system on the right. The upper images show the system with a protein-to-lipid ratio of 1 : 50 in each leaflet, and the lower ones the case with the protein-to-lipid ratio of 1 : 100 per leaflet. In each case, the simulated system has been repeated four times (2 × 2) with periodic boundary conditions to better visualize large-scale ordering. Snapshots correspond to the end of each respective simulation. Proteins are colored in yellow and lipids in brown. Pictures have been rendered with VMD.

Table 1 Details of the simulated protein–lipid systems. "A" stands for aggregating, "NA" for non-aggregating, and "INF" stands for infinity. The number of proteins refers to the total number in the bilayer. The number of lipids in the 1 : INF system is 2045 (DPPC) or 3000 (DLPC)

DPPC (A)						
Protein-to-lipid ratio	1 : 50	1 : 75	1 : 100	1 : 150	1 : 200	1 : INF
No. of proteins	16	16	9	9	4	1
Size in *x*/*y* (nm)	27.4	31.3	26.1	30.9	23.4	25.1
Size in *z* (nm)	9.5	9.3	9.5	9.3	9.6	9.4
DLPC (NA)						
Protein-to-lipid ratio	1 : 50	1 : 75	1 : 100	1 : 150	1 : 200	1 : INF
No. of proteins	16	16	9	9	4	1
Size in *x*/*y* (nm)	27.2	31.2	26.1	30.7	23.3	30.1
Size in *z* (nm)	9.3	9.4	9.2	9.3	9.2	9.1

contained one, four, nine, or sixteen proteins depending on the protein-to-lipid ratio. For comparison with experimental studies, the surface area covered by proteins was in the different DPPC–NaK systems as follows: 2.4% (1 : infinity), 11% (1 : 200), 15% (1 : 150), 21% (1 : 100), 27% (1 : 75), and 34% (1 : 50). The system dimensions ranged between 23 and 31 nm along the bilayer (*xy*-plane). The thickness of the system along membrane normal direction (*z*) was about 10 nm. These values are listed in Table 1.

The molecules were modelled with a CG force field derived from MARTINI[51–53] and modified for membrane peptides and proteins.[54] The starting structure of the

protein was also based on the earlier work discussed elsewhere.[54] The simulations were carried out using the GROMACS simulation package.[47] The A-systems were simulated for 26 μs and the NA-systems for 10 μs. Data were collected every 100 ps. The time step was fixed to 40 fs in all simulations. Data corresponding to the first microsecond of simulation were discarded in all diffusion analysis to account for equilibration. Below, the time scales reported for the CG models are the real simulation times without a commonly used scaling factor of four[51–53] that is used to account for the faster dynamics in CG models compared to atomistic ones. However, the diffusion coefficients reported below have been scaled by this factor.

The electrostatics were handled by potentials shifted to zero in the interval from 0 to 1.2 nm. The Lennard-Jones interactions were shifted in between 0.9 and 1.2 nm. Neighbor lists with a radius of 1.2 nm were updated every 10 steps. NPT ensemble was adapted and pressure was held constant at 1 bar with the Parrinello–Rahman barostat[55] with a time constant of 4 ps and compressibility of 4×10^{-5} bar^{-1}. The x and y directions were coupled together and z separately. The system was also coupled to a heat bath at 310 K produced by the Nosé–Hoover thermostat[48] with a time constant of 1 ps. No constraints were applied to the bonds.

2.3 Mean-squared displacement

The mean-squared displacement (MSD) curves act as a starting point for the diffusion analysis. The MSD can be calculated as

$$\mathrm{MSD}(t) = \langle [\mathbf{r}_i(t + t') - \mathbf{r}_i(t')]^2 \rangle, \quad (1)$$

where $\mathbf{r}_i(t)$ is the location of the examined particle i at time t. Angular brackets denote averaging over both time and the set of examined particles. Lateral diffusion coefficient describing the pace of motion in the xy (membrane) plane is obtained from the MSD as

$$D_L = \lim_{t \to \infty} \frac{\mathrm{MSD}(t)}{4t}. \quad (2)$$

The MSD in eqn (1) is based on a time average taken over the time series $\mathbf{r}(t)$ of the lipid motion. While viscoelastic subdiffusion is ergodic in the sense that in the limit of long measurement times the ensemble average and the time average of the MSD are identical for free motion[56–58] (in contrast to anomalous diffusion with scale-free waiting time distributions[59] as observed in ref. 15), for finite measurement times the amplitude of the time averaged MSD fluctuates around the ergodic value.[57] A smooth curve may be obtained by averaging the time averaged MSD over individual trajectories. Further, it is important to mention that the long-time limit in eqn (2) means that D_L should be determined from the region where $\mathrm{MSD}(t) \sim t^{\alpha}$ with $\alpha = 1$.

In Langmuir monolayers, the MSD curves were computed for the 90 phospholipid molecules in each monolayer (diffusion of cholesterol was not included in the analysis). The two monolayers in each system (separated by vacuum) were considered independently, and the motion of the centre of mass (COM) of the examined monolayer was discarded before the analysis. This choice was made to avoid possible issues, which could arise from the motion of the leaflet as a whole,[60,61] and therefore, in practice, the motion of each lipid's COM was determined with respect to the center of mass of the monolayer in which the given lipid resides. Data used in further analysis were based on an average of MSD results of the two monolayers.

In protein–bilayer systems, the integral proteins anchor the leaflets to one another, and hence the possible motion of the two bilayer leaflet COMs (compared to each other) is expected to be much slower compared to membrane protein-free systems. Given this, in bilayer systems we first removed the COM motion of the membrane

(by accounting for all lipids and proteins, but not water) and then determined the displacements of particles' COM to compute the MSDs.

2.4 Exponent associated with mean-squared displacement

We assume the mean-squared displacement to scale as a power-law in time as follows:

$$\mathrm{MSD}(t) \sim t^{\alpha}, \tag{3}$$

where $\alpha = \alpha(t)$ is the time-dependent anomalous diffusion exponent. By definition, the exponent can be obtained as the slope of log(MSD) *versus* log(t). In practice, the MSD data are first translated to a logarithmic scale. However, as particle locations are sampled at constant time intervals in our simulations, the data obtained are not uniformly spaced in the logarithmic description. To fix this issue for further analysis, a smoothing spline was fitted to the log–log data and the spline was sampled at constant intervals in the logarithmic scale. This fitting procedure also smoothed roughness in the data which occurs when data saved from different sets of simulations with different saving frequencies overlap.

The time dependence of α was calculated by fitting a straight line to a moving window containing 20 data points (represented in a log–log scale) both backward and forward of the examined moment of time. This interval corresponds to 0.41 time units in logarithmic scale with a base of 10.

In a further step the anomalous motion should be scrutinised through additional, complementary analysis tools to diagnose precisely the nature of the stochastic motion of lipids and proteins. For instance, one may analyse moment ratios,[62] the velocity autocorrelation,[57] or apply the p-variation method.[63] The results of analysis based on these tools will be discussed elsewhere.

3 Results

3.1 Diffusion in Langmuir monolayers

The MSD curves obtained from the longest simulations are shown in Fig. 3. The data of the most compressed and the most expanded systems have been calculated from the whole trajectory (>600 ns), resulting in better statistical quality compared to the other cases where simulations lasted for 100 ns. Still, in all cases the MSD data are fairly smooth.

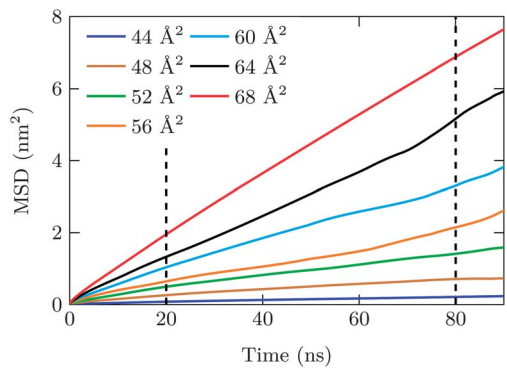

Fig. 3 MSD curves of phospholipids in the monolayer systems, with colors corresponding to different compression states. Dashed lines show the time range used in fitting eqn (2) to the data.

The data in Fig. 3 bring about a very important point which one should pay attention to in all the discussion below. That is, the MSDs in Fig. 3 are *seemingly linear in time*, therefore supporting the idea that one could use eqn (2) to determine the diffusion coefficient. However, as the data and the discussion below show, this is not the case. Nonetheless, for the time being, let us assume that the assumption of MSD(t) $\sim$ t^1 holds. Possible issues related to the calculation of the diffusion coefficient when the exponent is less than one will be addressed and discussed later in the Discussion.

The diffusion coefficients obtained from fitting eqn (2) to the MSD data are shown in Fig. 4. The diffusion coefficients are consistent with the expected behavior that lipid dynamics are faster the looser the packing in a monolayer. The diffusion coefficients are also in agreement with experimentally and computationally measured values for lipid diffusion in monolayers, if the effect of cholesterol is taken into account (see discussion in ref. 43). Notably, even in the most packed system (44 Å^2) the diffusion coefficient is several orders of magnitude larger compared to diffusion in the gel (solid-like) phase, where diffusion coefficients in lipid bilayers are[1] of the order of 10^{-16}–10^{-11} cm^2 s^{-1}, highlighting that all systems considered here are fluid.

3.2 Self-assembly of membrane proteins in bilayers

Before considering lateral diffusion in lipid bilayers with membrane proteins, it is crucial to have well-defined systems that have equilibrated. To this end, the aggregation tendency of membrane proteins was investigated by calculating the number of close contacts between proteins during the simulations. The calculation was performed every 100 ns, analyzing the first 10 μs of all systems. Two proteins were considered to be in close contact if the distance between their centres of mass in the *xy*-plane was smaller than 1.7 times the initial maximum distance between the beads of a protein and its COM. While protein radius is not easy to define, according to our benchmarks on the validity of the chosen criterion, the chosen value was found to best describe the limit at which there is a contact between two proteins. The calculated aggregation maps are shown in Fig. 5.

The results (Fig. 5) confirm the conclusion which was readily hinted by Fig. 2: proteins in A-systems start to form aggregates already after a few hundred nanoseconds and almost all proteins become connected to each other during the first microsecond. The clusters of proteins are also stable in the A-system. This result also supports our choice to discard the first microsecond of simulation data from the analysis as the formation of protein aggregates takes about a microsecond.

In the NA-system, proteins tend to stay unconnected for up to microseconds and some of them remain separated from other proteins during the whole 10 μs

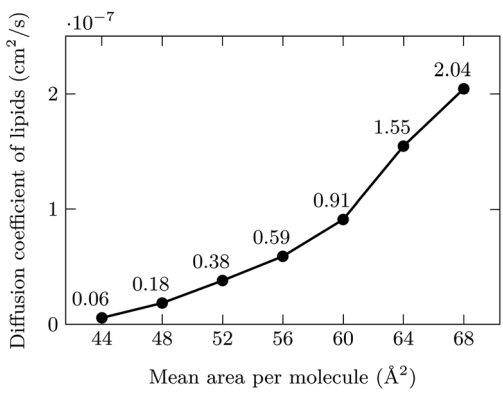

Fig. 4 Diffusion coefficients of phospholipids in Langmuir monolayer systems as a function of mean area per molecule.

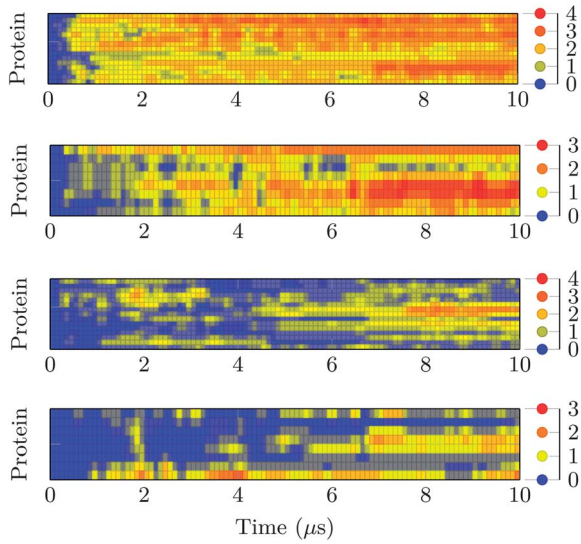

Fig. 5 The number of close contacts that each protein has with other proteins. The two upper figures show the behavior in the aggregating DPPC system (A) with protein-to-lipid ratios of 1 : 75 (top) and 1 : 100 (second from top). The two lower plots show the number of close contacts in the non-aggregating DLPC system (NA) with similar protein-to-lipid ratios of 1 : 75 (second from bottom) and 1 : 100 (bottom). Note that the color bars are scaled differently in systems with a different total number of proteins.

simulation. The aggregates in the NA-system are also able to break apart once they are formed.

The difference in protein behavior between the two lipid–protein systems, and especially the time it takes to form aggregates, cannot be explained by the speed of lateral dynamics. The proteins in DLPC (NA) membranes have higher diffusion coefficients compared to the DPPC (A) membranes (data to be shown below), thus in the NA-systems the proteins meet other proteins on time scales shorter than those in the A-systems. Yet, the aggregates form faster in the A-systems, which confirms the higher aggregation tendency of proteins in the DPPC bilayer.

3.3 Diffusion in aggregating (A) protein system

With the first microsecond of data discarded, a total of 25 μs of simulation time was considered for MSD calculation of the aggregating NaK–DPPC system. The MSD curves for lipids are shown in Fig. 6 and for proteins in Fig. 7.

Fig. 6 suggests that the dynamics of lipids are faster in the less crowded systems, as expected. Diffusion slows down even for minor protein concentrations, and this effect is the stronger the larger is the concentration of proteins.

The effect of crowding on protein motion is even more dramatic than in the case of lipids, see Fig. 7. The system with a protein-to-lipid ratio of 1 : 200 shows a drastic slowing down of diffusion.

The lipid diffusion coefficients determined from the MSD curves with different levels of crowding are listed in Fig. 8. The diffusion coefficients decrease almost linearly with increasing protein-to-lipid ratio. The decrease arises in part from the effect of blocking: as the protein content increases, there is less space for lipid motion, slowing down diffusion. Confinement of lipids in cages formed by proteins strengthens this effect (see Fig. 2), and it is likely that lipid–protein interactions play a role, too. In experiments, in line with our data, proteins have been found to cause a significant reduction in lateral diffusion rate of phospholipids in the plane of membranes.[8]

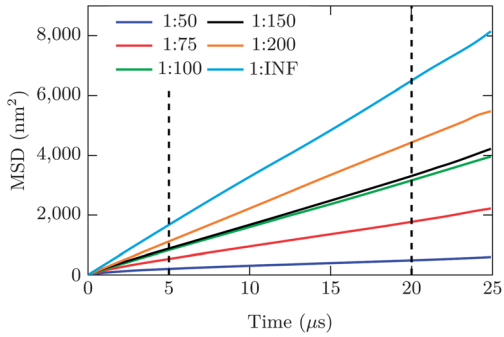

Fig. 6 MSD curves of lipids in the DPPC (A) systems with different protein-to-lipid ratios. Dashed lines show the time range used in fitting eqn (2) to the data.

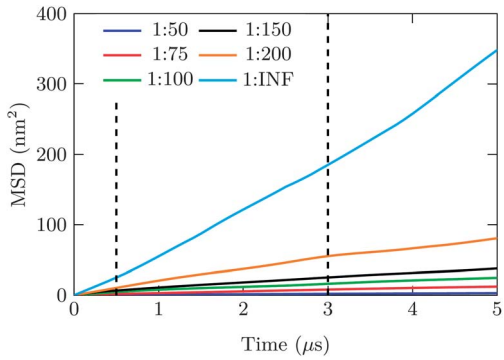

Fig. 7 MSD curves of proteins in the DPPC (A) systems. The time range used for fitting eqn (2) is shown with a pair of dashed lines.

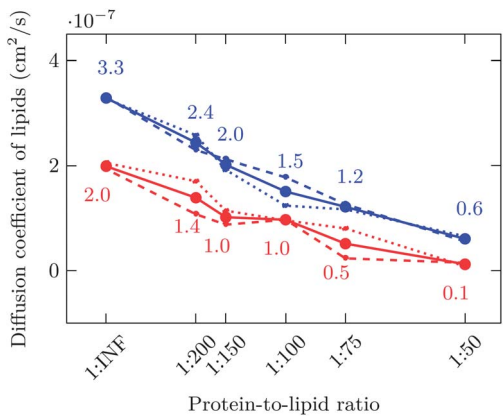

Fig. 8 Diffusion coefficients of lipids in membranes with different protein-to-lipid ratios: data for DPPC (red) and DLPC (blue). INF stands for infinity. The diffusion coefficients in x and y directions have been drawn with dashed and dotted lines of the same color, respectively, full curve being the average.

The values for the diffusion coefficient in x and y directions were also calculated in order to examine the possible anisotropic effects of wall-like structures formed by protein aggregation. These coefficients are also shown in Fig. 8. Not surprisingly,

in some systems lateral diffusion is not uniform in both directions in the plane. These differences in x and y directions may also in part be due to finite size effects. However, the differences are relatively small.

The diffusion of proteins is even more affected by crowding, see Fig. 9. First, for the aggregating proteins, the dependence of protein diffusion coefficient on protein-to-lipid ratio is stronger than linear. Second, its values span two orders of magnitude in the case of the DPPC (A) system. A seemingly minor increase in protein content from 1 : infinity to 1 : 200 slows diffusion down by a factor of four. In the most crowded DPPC–NaK system protein motion has virtually stopped, which is described by a very low value of the diffusion coefficient (about 1×10^{-10} cm^2 s^{-1}). When the diffusion coefficients of lipids and proteins are compared to each other, the diffusion of proteins is slower by a factor of 5 (protein-poor) to 30 (protein-rich conditions).

If the diffusion of membrane proteins could be described in terms of hard disks moving on a plane, then the protein diffusion coefficient would decrease linearly for increasing area fraction covered by proteins.[64] Based on Fig. 9, this behavior holds approximately well at small protein-to-lipid ratios but breaks down around 1 : 150, where protein clustering becomes evident. Clearly, aggregation of proteins plays a profound role in protein diffusion under crowding, and theoretical work to describe this behavior would be welcome.

Experiments have shown quite generally that the lateral diffusion coefficient of membrane proteins decreases for increasing protein concentration,[32,37,65] in agreement with our data.

3.4 Diffusion in non-aggregating (NA) protein systems

The analysis on the non-aggregating protein–DLPC system was performed similarly as on the aggregating protein–DPPC system. The diffusion coefficients are depicted in Fig. 8 and 9.

Diffusion coefficients of lipids in the non-aggregating systems are 1.5 to 5 times higher than the values in the aggregating DPPC membranes. In the limit of small protein concentration (1 : infinity), aggregation of proteins cannot affect lipid diffusion, thus the main reason why DLPC and DPPC diffuse at a different pace in this limit is the different viscosity (or alternatively a different membrane fluidity described also by a different average area per lipid) of these lipid bilayers. If changes in membrane viscosities are assumed to be similar in DPPC and DLPC bilayers with

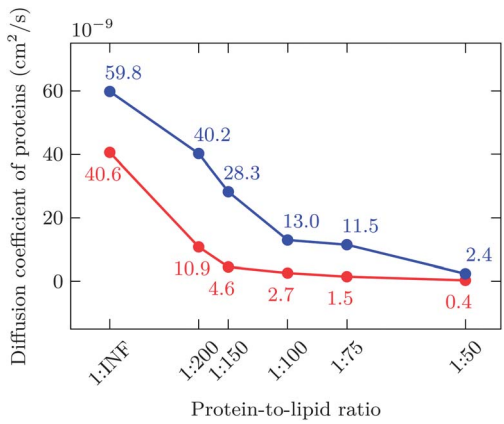

Fig. 9 Diffusion coefficients of NaK channel proteins in membranes with different protein-to-lipid ratios. Curves show lateral diffusion coefficients in DPPC (red) and DLPC membranes (blue). INF stands for infinity.

increasing protein density, then in the 1 : 50 ratio, the diffusion of DPPC is slowed down by a factor of 3.6 compared to DLPC, and this difference is due to protein aggregation.

Protein diffusion in the DPPC system is slowed down by a factor of 1.5 to 10 compared to DLPC, as the protein-to-lipid ratio is increased from 1 : infinity to 1 : 50, respectively. Again in the dilute protein system, the difference in protein diffusion coefficients is due to different membrane viscosities in the DLPC and DPPC bilayers. The remaining part is due to aggregation, or changes in membrane viscosity associated with aggregation.

3.5 Anomalous diffusion exponent

3.5.1 Langmuir monolayer systems. As data on lipid diffusion in Langmuir monolayers were collected in multiple simulations with different data saving intervals, it was first combined for the log–log plots. The smoothed data, spanning almost 8 orders of magnitude, are shown in Fig. 10.

We can readily find three different regimes in Fig. 10. First, there is a regime corresponding to superdiffusive ballistic motion at very short time scales. In this regime, the exponent $\alpha = 2$. Anomalous diffusion follows after a transition period and is characterized by an exponent smaller than one. Finally, at long times, one finds a transition towards normal diffusion characterized by an exponent $\alpha = 1$.

For further analysis, let us focus on how α behaves in time, see Fig. 11. It is readily seen that the level of compression has a profound effect on the nature of diffusive motion. At very short times the behavior in the monolayers subject to different packing conditions is similar, characterizing ballistic motion. However, the curves describing different packing conditions start to separate from each other in a time scale of hundreds of femtoseconds.

Subsequently, superdiffusion changes into subdiffusion in about 1 picosecond, and one finds a plateau consistent with subdiffusion with an exponent that is approximately constant over several orders of magnitude in time, starting between 1 and 10 picoseconds. The subdiffusion exponents of the most compressed and the most expanded systems were found to be quite low: 0.30 and 0.57, respectively. The tighter the packing, the smaller the exponent.

After the subdiffusive regime, the exponents start to grow, expected to level off at a value of one, thus describing normal random walk like diffusion at long times. In the most expanded system the long-time regime was almost reached during the simulations, and one can estimate that the onset of normal diffusion (τ_{onset}) in this case is

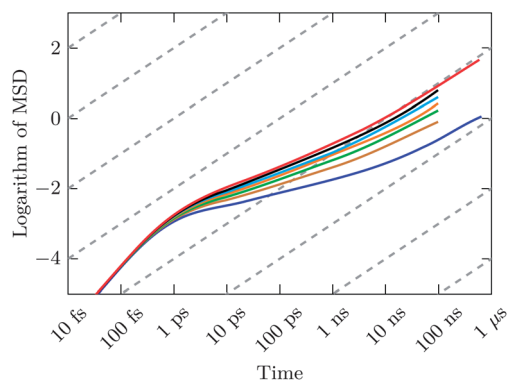

Fig. 10 Mean-squared displacements of lipids in Langmuir monolayers shown on a log–log scale. The dashed gray lines show normal diffusion behavior with $\alpha = 1$. Color code used in the curves is as follows: 44 Å^2 (blue), 48 Å^2 (brown), 52 Å^2 (green), 56 Å^2 (orange), 60 Å^2 (cyan), 64 Å^2 (black), and 68 Å^2 (red).

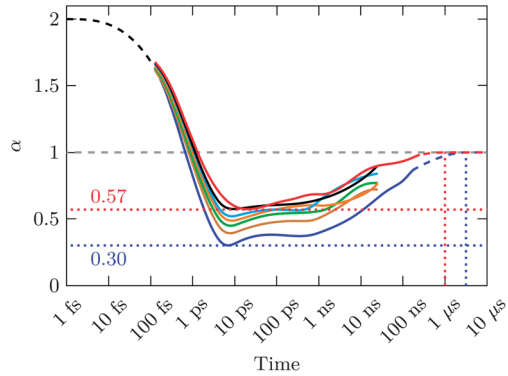

Fig. 11 Time evolution of the exponent α associated with the mean-squared displacement of lipids in Langmuir monolayers. Color code used in the curves is as follows: 44 Å^2 (blue), 48 Å^2 (brown), 52 Å^2 (green), 56 Å^2 (orange), 60 Å^2 (cyan), 64 Å^2 (black), and 68 Å^2 (red). Dashed black line shows the expected extrapolation to ballistic behaviour ($\alpha = 2$), and the dashed red and blue lines show extrapolation to normal diffusion ($\alpha = 1$) at long times. Dotted red and blue lines guide the eye to the estimated time scales in which normal diffusion is reached, and also to the subdiffusion exponent. Dashed gray line shows the normal diffusion exponent. Error bars (considering the standard error of the mean) in the value of α are very small at short times (± 0.01) and increase slightly at longer times (± 0.03).

close to 1 microsecond. Other, more compressed systems are expected to behave similarly but less rapidly, and our best educated guess based on the data in Fig. 11 suggests that the onset of normal diffusion ranges in these cases from about 1 to 10 microseconds.

3.5.2 Aggregating protein systems. For the DPPC system with protein aggregation, the time evolution of α for lipid motion is shown in Fig. 12. The corresponding curve for protein diffusion is depicted in Fig. 13.

We stress that the data in this case have been collected at fairly long intervals of 100 picoseconds in order to focus on the long-time motion. Therefore, a plateau associated with subdiffusion is not included in Fig. 12 and 13 (compared to Fig. 11). It would appear at short times (<1 ns) if data of particle positions had been saved more frequently.

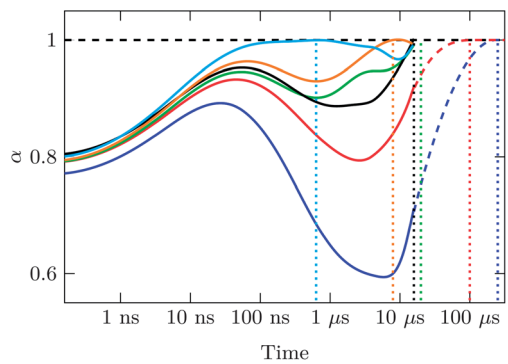

Fig. 12 Exponent characterizing lipid motion in the aggregating DPPC systems. Curves are colored as follows: 1 : 50 (blue), 1 : 75 (red), 1 : 100 (green), 1 : 150 (black), 1 : 200 (orange), and 1 : infinity (cyan). Error bars (considering the standard error of the mean) in the value of α are the smallest at short times (<0.01) and increase up to about ± 0.01 at 3 μs. Extrapolations at the longest times (shown by dashed lines) are based on a conservative estimate of $\alpha(t)$ between about 10–20 μs.

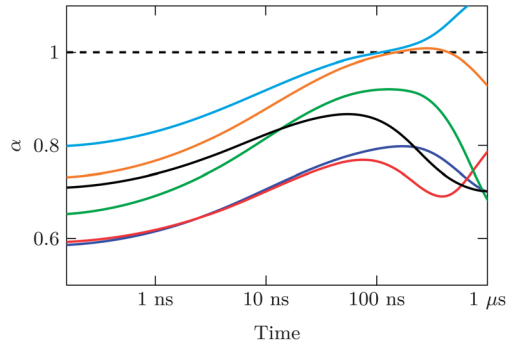

Fig. 13 Exponent characterizing protein motion in the aggregating DPPC systems. Curves are colored as follows: 1 : 50 (blue), 1 : 75 (red), 1 : 100 (green), 1 : 150 (black), 1 : 200 (orange), and 1:infinity (cyan). Error bars are about ±0.01 at short times and about ±0.02 at the longest times.

Let us first focus on lipid motion (Fig. 12). At times of the order of 1–100 ns, the exponent in every case increases towards one, reflecting a tendency to aim for random walk like motion. In the most dilute system with just a single membrane protein, the regime of normal diffusion is indeed reached in about 100 ns. However, in other systems where crowding of proteins becomes more prominent, the exponent falls down and reaches a minimum at 1–10 μs, the exponent being the smaller the more crowded the membrane is, and the time at which the minimum is observed increasing for increasing crowding. We discuss this in more detail below.

The collisions of lipids with proteins become more and more frequent for increasing protein concentration, giving rise to dynamical correlations in lipid motion, which in turn is manifested as anomalous diffusion ($\alpha < 1$) where the motion of lipids has a memory. We find that the anomalous diffusion exponent decreases for increasing protein concentration, in agreement with experiments by Horton *et al.*[66] At very long times the lipids will undergo a random walk characterized by $\alpha = 1$, and therefore one can expect the curves in Fig. 12 to eventually recover to a value of one. How long this takes is not clear, though. The data in Fig. 12 suggest that for intermediate crowding (1 : 200, 1 : 150, 1 : 100) normal diffusion would be observed at times of the order of 10 μs. For the most crowded systems (1 : 75, 1 : 50), the time scale of reaching normal diffusion is considerably larger, and our best educated guess based on interpolation of the data is that normal diffusion would be observed at times of the order of 100 μs or even milliseconds.

Let us come back to Fig. 12 and discuss why the anomalous diffusion exponent decreases at intermediate times. The data below (Fig. 16) for the non-aggregated lipid–protein system do not highlight a similar major decrease in α, thus the drop in the exponent cannot be due to lipid–protein collisions as such. Instead, it turned out that the decrease in α is largely due to lipids whose motion is confined due to proteins around them. As Fig. 2 shows, there are membrane regions where the lipids are surrounded by proteins from all possible directions, confining their motion to a limited part of the membrane. This is illustrated in Fig. 14, which shows a trajectory of a single tagged lipid during a 25 μs simulation. The motion of the lipid is clearly restricted, allowing it to access only part of the membrane surface. If the confinement would continue over a period longer than the simulation time, then MSD would converge to a constant value, implying that one would have a situation where $\mathrm{MSD}(t) \sim t^0$. The data in Fig. 12 suggest that the waiting time of lipids to escape confined regions is large, but it is smaller than the simulation time. This is also supported by the data in Fig. 15, which depicts time-averaged MSDs of all lipids in the DPPC system one by one, and, more importantly, the distribution of the single-particle-based anomalous diffusion exponents at times of 10 ns and 1 μs. The

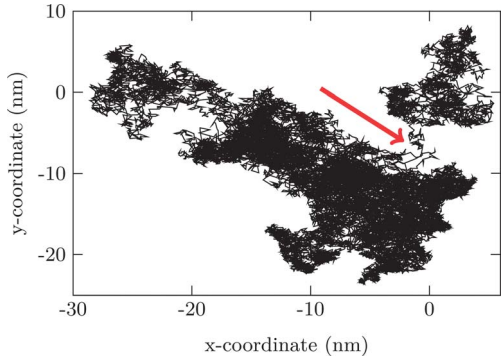

Fig. 14 Trajectory of a single tagged lipid in the DPPC–NaK system with a protein-to-lipid ratio of 1 : 50 over a simulation time of 25 μs. Note confinement of the lipid into restricted areas. The red arrow shows how the lipid escapes from one region, ending up in another, moving through a narrow channel between the two.

distribution of α in both cases is quite broad, but importantly in the latter case (at 1 μs) there are no or just a few exponents close to zero but there are exponents equal to one. In other words, the data indicate that while there are few lipids whose motion is almost non-existent due to the caging effect of proteins, the confinement of lipids is temporary. Also, at times of the order of a microsecond there are individual lipids undergoing free random walk like diffusion.

In the case of protein motion, Fig. 13 demonstrates that the conclusions based on lipid motion are largely valid also for protein motion. The main differences are the smaller exponent values in protein motion, and the time scales that seem to be longer for proteins compared to lipids. That is, normal diffusion is recovered in non-crowded systems in about one microsecond, but in the highly crowded cases the time required for accessing the normal diffusion regime is likely larger than in the case of lipid motion.

3.5.3 Non-aggregating protein systems. In the non-aggregating DLPC–protein systems, the time evolution of α for lipids is shown in Fig. 16. As it shows, the nature of lipid diffusion in the non-aggregating protein system is somewhat different compared to that of the aggregating DPPC system. Unlike in the DPPC–NaK system (Fig. 12), here the dip in the exponent α is much less evident. Instead, there

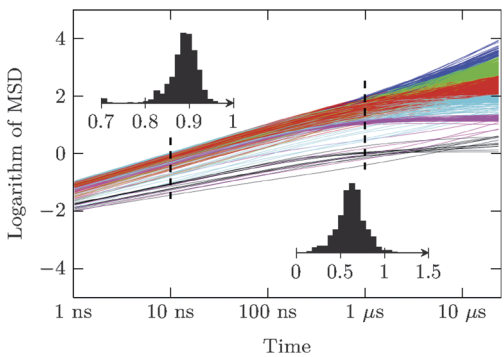

Fig. 15 MSDs shown separately for each lipid in the DPPC–NaK system with a protein-to-lipid ratio of 1 : 50. Also shown in insets are the distributions of anomalous diffusion exponents at two different times (10 ns and 1 μs) to demonstrate their width and approximate Gaussian profile.

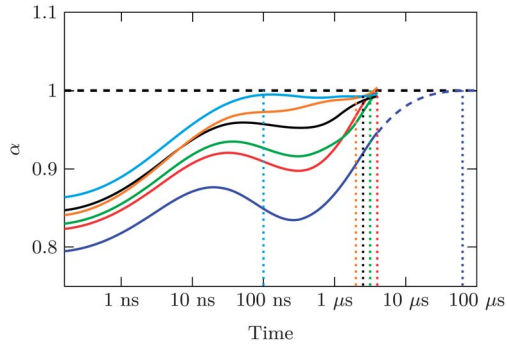

Fig. 16 Exponents determined from running fits for the MSD of lipids in non-aggregating DLPC–protein systems. Curves are colored as in earlier plots: 1 : 50 (blue), 1 : 75 (red), 1 : 100 (green), 1 : 150 (black), 1 : 200 (orange), and 1 : infinity (cyan). Normal diffusion behavior with $\alpha = 1$ is shown with a gray dashed line. Error bars are as in Fig. 12. Extrapolation at long times (shown by a dashed line) in the 1 : 50 case is based on a conservative estimate of $\alpha(t)$ between 1–5 μs.

is almost a plateau covering about one order of magnitude in time from a few tens of nanoseconds to a few hundred nanoseconds. The plateau is a common feature in all non-aggregating systems. The system with a single protein (1 : infinity) finds the normal diffusion regime in about 100 ns, whereas in the multi-protein systems the diffusion becomes normal with $\alpha = 1$ at much longer times. Even minor crowding (1 : 200) increases the onset of normal diffusion to about 1 μs. In more crowded systems it is more difficult to estimate how long it takes to get to the normal diffusion regime, but, again based on an educated guess, it ranges roughly between 10 and 100 microseconds.

Importantly, in the dilute case (1 : infinity) the time dependence of α in the aggregating and non-aggregating systems is almost identical (see Fig. 12 and 16). The differences between the DLPC–protein and DPPC–protein systems under crowding are therefore not due to different dynamics of the lipid molecules but rather result from alterations caused by the aggregation tendency of the proteins. Furthermore, also important to stress is that atomistic Langmuir monolayer simulations and coarse-grained lipid bilayer models are largely consistent with each other: in Langmuir monolayers with an area per lipid comparable to tensionless lipid bilayers (60–68 Å^2), normal diffusion is accessed in 100–1000 ns, which is also the case in coarse-

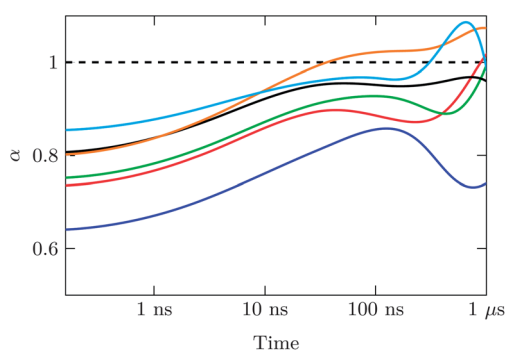

Fig. 17 Exponents determined from running fits for the MSD of proteins in non-aggregating DLPC–protein systems. Curves are colored as in earlier plots: 1 : 50 (blue), 1 : 75 (red), 1 : 100 (green), 1 : 150 (black), 1 : 200 (orange), and 1 : infinity (cyan). Normal diffusion behavior with $\alpha = 1$ is shown with a gray dashed line. Error bars are as in Fig. 13.

grained model studies. The time scales predicted by the coarse-grained models are therefore in the right ballpark (regarding the order of magnitude).

The plots for protein motion, see Fig. 17, show slightly different behavior compared to the aggregating system (Fig. 13). The diffusion exponents α for DLPC–protein membranes are larger than in the case of the aggregating DPPC system and they reach $\alpha = 1$ to some extent faster.

4 Discussion and conclusions

Cell membranes modulate or even govern a variety of cellular functions. The key molecules either responsible or at least involved in these functions are lipids and membrane proteins. To understand their full role in cellular functions, one has to understand the principles that control their lateral dynamics as the formation of functional nanoscale membrane domains (with a specific set of proteins and lipids) is based on lateral diffusion. However, while this dynamical process has been paid a great deal of attention to, most of the previous studies have been based on rather idealized conditions where the complexity of native membranes has not been taken into account. One of the great challenges in this spirit is to understand the effects of crowding on lipid and protein diffusion.

Here we have considered this topic from two complementary viewpoints, elucidating the effects of lipid packing through considerations of Langmuir monolayers, as well as the effects of protein crowding in lipid bilayers.

Simulations of Langmuir monolayers in the absence of proteins indicated that the motion of lipids is to do with quite substantial memory effects manifested as anomalous diffusion that persist over a broad range of time. We observed that the anomalous diffusion exponent depends on the packing of the monolayer; increasing packing leading to smaller exponent. In the same spirit, also the transition from anomalous to normal diffusion was found to depend on how strongly the lipids are packed, as increasing packing increases the onset of normal (random walk like) diffusion. What is quite stunning is the magnitude of the characteristic time needed to cross over from anomalous to normal diffusion (τ_{onset}). Even in fluid monolayers where packing of lipids is low (like in the liquid-expanded phase), τ_{onset} was found to be several hundred nanoseconds, and in the most compact monolayers of the order of microseconds.

In simulations of lipid bilayers the objective was to further our understanding of proteins' role in lateral diffusion, when proteins either aggregate or stay apart from each other. We observed the influence of protein crowding on lateral diffusion to be strong. Increasing protein concentration slowed down both lipid and protein diffusion, the slowing down being as large as a factor of 10 for lipids and 20–100 for proteins. Recent simulation results by Domanski *et al.* are consistent with this picture.[38] We also explored the extent to which protein crowding can affect τ_{onset}, thereby slowing down lateral dynamics. The observed effects associated with anomalous diffusion demonstrated the roles of blocking (entropy) and protein self-organization (aggregation). The system that promoted protein aggregation expressed the strongest effects manifested as lipid and protein confinement, complemented by the largest values we observed for τ_{onset}.

All simulated scenarios point to the fact that in systems that are highly packed or crowded with proteins, the time it takes to access the regime of normal diffusion is large. In protein-poor systems this ranges from 100 to 1000 ns. In protein-rich systems with significant crowding, τ_{onset} can be of the order of milliseconds. Experiments using biotinylated avidin lipid anchors as a crowding agent suggest[66] that τ_{onset} could actually be much larger, of the order of 100 ms. Is this a potential problem? In simulations it is, since availability of computer resources needed to access millisecond simulations are not common. If one wanted to explore lipid and/or protein diffusion in native-like membranes with a significant concentration of proteins, one should carry out simulations that last for several milliseconds.

Shorter simulations would not provide quantitatively reliable data for normal diffusion. This stems from the fact that the definition of the lateral diffusion coefficient is valid only in the limit of long times (see eqn (2)) for random walk like diffusion, when $\alpha = 1$. If $\alpha < 1$, as in anomalous diffusion, the diffusion coefficient is not well defined. This is the case, *e.g.*, when the simulation time is less than τ_{onset}. In practice the simulation time should however be considerably longer, at least $10 \times \tau_{onset}$, to gather decent statistics for MSD up to times that are much longer than the onset of normal diffusion τ_{onset}.

The above implies that the reader should consider our data for diffusion coefficients with reservation, too. Despite our best efforts and quite substantial computer resources, even the longest of our simulations covered less than 30 microseconds. Therefore, at least the diffusion coefficients of the most crowded protein systems (1 : 50, 1 : 75, and 1 : 100) studied in this work are questionable. Quite likely they are qualitatively in order, but quantitatively they are certainly compromised since in those cases we were not able to gauge the times where $\alpha = 1$.

What is even more stunning are the conclusions of our atomistic Langmuir monolayer simulations, which set the minimal standard for atomistic simulations of lipid diffusion in fluid membranes: the simulations should last at least for 1000 ns. This is not good news given that the simulation time scale of typical atomistic MD simulations of lipid membranes is currently of the order of 100 ns. Of course, one can use such data for consideration of lateral diffusion, and one can extract the diffusion coefficient too, but one should keep in mind that the quantity obtained in this manner will be an effective one, describing subdiffusive behavior instead of long-time (hydrodynamic) normal diffusion. The comparison of subdiffusive data determined from simulations with long-time scale diffusion data measured in experiments would also be problematic, and comparison of trends would then be more meaningful instead of comparing just quantitative numbers.

Quite unfortunately, the above scenario is yet the optimistic one, if one considers the challenge to simulate long enough times. The above discussed views hold as long as the lipids and proteins diffuse in a well-defined membrane domain. If the membrane is characterized by formation of domains with different properties, or if there is a need to consider diffusion in a membrane coupled to an actin-based membrane skeleton, then one has to account for effects of domain boundaries that typically slow down diffusion from one domain to another. The hydrodynamic long-time diffusion would then take place at times much larger than those associated with diffusion inside a single membrane domain. It is quite plausible that if one wanted to consider lateral diffusion of proteins in heterogeneous membranes with considerable domain formation, including the effects of actin-based confinement, then the true normal diffusion in the hydrodynamic long-time limit would be observed only in simulations of the order of seconds or minutes. While these time scales are just an educated guess, they highlight the size of the challenge.

Finally, let us briefly discuss physical limits of protein motion. Following the ideas of Dill *et al.*, is there an optimal concentration of membrane proteins that would maximize the speed of biochemical reactions?[67] On the one hand, protein diffusion should then be fast enough to enable sufficiently rapid motion over large length scales. This idea would be best fulfilled in protein-poor membranes. On the other hand, the optimal conditions should also promote protein–protein collisions needed for protein complex formation, and this idea in turn would favor crowding. Using hard sphere models for proteins in cytosol, Dill *et al.* predicted that the optimal protein volume concentration would be 19%, compared to 20% observed in cells.[67] In 2D membranes the validity of the hard disk model is less obvious, but what is obvious is that the protein concentration cannot be too high, since otherwise protein diffusion would become too slow as the data in Fig. 9 also demonstrate. Actually, what is striking in Fig. 9 is the slowing down of diffusion in the aggregating DPPC–NaK system, where protein diffusion slows down rather steeply down to a protein-to-lipid ratio of 1 : 150. This corresponds to an area fraction of 15%

occupied by the proteins. Similar diffusion in the non-aggregated DLPC–NaK system is observed with the protein-to-lipid ratio of 1 : 50, corresponding to a protein area fraction of 34%. If cells want to maximize their membrane protein diffusion without sacrificing chances for biochemical reactions (in terms of protein complex formation), then our data suggest that protein concentration is anything but constant in the membrane plane but is strongly dependent on proteins' preference for aggregation.

Acknowledgements

We acknowledge Mark Sansom and Phillip Stansfeld for sharing their membrane protein models. We wish to thank CSC – IT Centre for Science (Espoo, Finland) for computing resources. The Academy of Finland and the European Research Council (project 290974 CROWDED-PRO-LIPIDS) is acknowledged for financial support.

References

1 P. F. F. Almeida and W. L. C. Vaz, *Handbook of Biological Physics*, Elsevier, Amsterdam, 1995, ch. 6, pp. 305–357.
2 I. Vattulainen and O. G. Mouritsen, *Diffusion in condensed matter: Methods, materials, models*, Springer-Verlag, Berlin, 2nd edn, 2005, pp. 471–509.
3 D. Lingwood and K. Simons, *Science*, 2010, **327**, 46–50.
4 E. Falck, M. Patra, M. Karttunen, M. T. Hyvonen and I. Vattulainen, *Biophys. J.*, 2004, **87**, 1076–1091.
5 P. S. Niemela, S. Ollila, M. T. Hyvonen, M. Karttunen and I. Vattulainen, *PLoS Comput. Biol.*, 2007, **3**, 304–312.
6 S. Ollila, M. T. Hyvonen and I. Vattulainen, *J. Phys. Chem. B*, 2007, **111**, 3139–3150.
7 A. Filippov, G. Oradd and G. Lindblom, *Biophys. J.*, 2007, **93**, 3182–3190.
8 J. B. de la Serna, G. Oradd, L. A. Bagatolli, A. C. Simonsen, D. Marsh, G. Lindblom and J. Perez-Gil, *Biophys. J.*, 2009, **97**, 1381–1389.
9 A. D. Dupuy and D. M. Engelman, *Proc. Natl. Acad. Sci. U. S. A.*, 2008, **105**, 2848.
10 K. Jacobson, O. G. Mouritsen and R. G. W. Anderson, *Nat. Cell Biol.*, 2007, **9**, 7.
11 T. A. Ryan, J. Myers, D. Holowska, B. Baird and W. W. Webb, *Science*, 1988, **239**, 61–64.
12 I. Golding and E. C. Cox, *Phys. Rev. Lett.*, 2006, **96**, 098102.
13 J.-H. Jeon, V. Tejedor, S. Burov, E. Barkai, C. Selhuber-Unkel, K. Berg-Sorensen, L. Oddershede and R. Metzler, *Phys. Rev. Lett.*, 2011, **106**, 048103.
14 R. Metzler and J. Klafter, *Phys. Rep.*, 2000, **339**, 1.
15 A. V. Weigel, B. Simon, M. M. Tamkun and D. Krapf, *Proc. Natl. Acad. Sci. U. S. A.*, 2011, **108**, 6438–6443.
16 S. Weber, A. J. Spakowicz and J. A. Theriot, *Phys. Rev. Lett.*, 2010, **104**, 238102.
17 J. Szymanski and M. Weiss, *Phys. Rev. Lett.*, 2009, **103**, 038102.
18 W. Pan, L. Filobelo, N. D. Q. Pham, O. Galkin, V. V. Uzunova and P. G. Vekilov, *Phys. Rev. Lett.*, 2009, **102**, 058101.
19 G. Guigas and M. Weiss, *Biophys. J.*, 2008, **94**, 90–94.
20 I. Bronstein, Y. Israel, E. Kepten, S. Mai, Y. Shav-Tal, E. Barkai and Y. Garini, *Phys. Rev. Lett.*, 2009, **103**, 018102.
21 M. A. Lomholt, I. M. Zaid and R. Metzler, *Phys. Rev. Lett.*, 2007, **98**, 200603.
22 I. M. Zaid, M. A. Lomholt and R. Metzler, *Biophys. J.*, 2009, **97**, 710–721.
23 E. Falck, T. Rog, M. Karttunen and I. Vattulainen, *J. Am. Chem. Soc.*, 2008, **130**, 44.
24 P. F. F. Almeida, W. L. C. Vaz and T. E. Thompson, *Biochemistry*, 1992, **31**, 6739–6747.
25 D. Turnbull and M. H. Cohen, *J. Chem. Phys.*, 1961, **34**, 120–125.
26 D. Turnbull and M. H. Cohen, *J. Chem. Phys.*, 1970, **52**, 3038–3041.
27 T. Apajalahti, P. Niemela, P. N. Govindan, M. S. Miettinen, E. Salonen, S. J. Marrink and I. Vattulainen, *Faraday Discuss.*, 2010, **144**, 411–430.
28 S. Busch, C. Smuda, L. C. Pardo and T. Unruh, *J. Am. Chem. Soc.*, 2010, **132**, 3232.
29 P. S. Niemela, M. Miettinen, L. Monticelli, H. Hammaren, P. Bjelkmar, T. Murtola, E. Lindahl and I. Vattulainen, *J. Am. Chem. Soc.*, 2010, **132**, 7574.
30 P. G. Saffman and M. Delbrück, *Proc. Natl. Acad. Sci. U. S. A.*, 1975, **72**, 3111–3113.
31 M. Weiss, H. Hashimoto and T. Nilsson, *Biophys. J.*, 2003, **84**, 4043.
32 M. Frick, K. Schmidt and B. J. Nichols, *Curr. Biol.*, 2007, **17**, 462–467.

33 S. Wieser, J. Weghuber, M. Sams, H. Stockinger and G. J. Schutz, *Soft Matter*, 2009, **5**, 3287–3294.
34 C. Eggeling, C. Ringemann, R. Medda, G. Schwarzmann, K. Sandhoff, S. Polyakova, V. N. Belov, B. Hein, C. von Middendorff, A. Schonle and S. W. Hell, *Nature*, 2009, **457**, 1159–1162.
35 K. Ritchie, X.-Y. Shan, J. Kondo, K. Iwasawa, T. Fujiwara and A. Kusumi, *Biophys. J.*, 2005, **88**, 2266–2277.
36 V. Mueller, C. Ringemann, A. Honigmann, G. Schwartzmann, R. Medda, M. Leutenegger, S. Polyakova, V. N. Belov, S. W. Hell and C. Eggeling, *Biophys. J.*, 2011, **101**, 1651–1660.
37 S. Ramadurai, A. Holt, V. Krasnikov, G. van den Bogaart, J. A. Killian and B. Poolman, *J. Am. Chem. Soc.*, 2009, **131**, 12650–12656.
38 J. Domanski, S. J. Marrink and L. V. Schafer, *Biochim. Biophys. Acta, Biomembr.*, 2012, **1818**, 984–994.
39 E. Flenner, J. Das, M. C. Rheinstadter and I. Kosztinh, *Phys. Rev. E*, 2009, **79**, 011907.
40 T. Akimoto, E. Yamamoto, K. Yasuoka, Y. Hirano and M. Yasui, *Phys. Rev. Lett.*, 2011, **107**, 178103.
41 G. R. Kneller, K. Baczynski and M. Pasenkiewicz-Gierula, *J. Chem. Phys.*, 2011, **135**, 141105.
42 R. Veldhuizen, K. Nag, S. Orgeig and F. Possmayer, *Biochim. Biophys. Acta, Mol. Basis Dis.*, 1998, **1408**, 90–108.
43 M. Javanainen, L. Monticelli, J. de la Serna and I. Vattulainen, *Langmuir*, 2010, **26**, 15436–15444.
44 O. Berger, O. Edholm and F. Jahnig, *Biophys. J.*, 1997, **72**, 2002–2013.
45 M. Holtje, T. Forster, B. Brandt, T. Engels, W. von Rybinski and H.-D. Holtje, *Biochim. Biophys. Acta, Biomembr.*, 2001, **1511**, 156–167.
46 W. L. Jorgensen, J. Chandrasekhar, J. D. Madura, R. W. Impey and M. L. Klein, *J. Chem. Phys.*, 1983, **79**, 926.
47 B. Hess, C. Kutzner, D. van der Spoel and E. Lindahl, *J. Chem. Theory Comput.*, 2008, **4**, 435–447.
48 D. J. Evans and B. L. Holian, *J. Chem. Phys.*, 1985, **83**, 4069.
49 T. Darden, D. York and L. Pedersen, *J. Chem. Phys.*, 1993, **98**, 10089.
50 B. Hess, H. Bekker, H. J. C. Berendsen and J. Fraaije, *J. Comput. Chem.*, 1997, **18**, 1463–1472.
51 S. J. Marrink, A. H. de Vries and A. E. Mark, *J. Phys. Chem. B*, 2004, **108**, 750–760.
52 S. J. Marrink, H. J. Risselada, S. Yefimov, D. P. Tieleman and A. H. de Vries, *J. Phys. Chem. B*, 2007, **111**, 7812–7824.
53 L. Monticelli, S. K. Kandasamy, X. Periole, R. G. Larson, D. P. Tieleman and S.-J. Marrink, *J. Chem. Theory Comput.*, 2008, **4**, 819–834.
54 M. Sansom, K. Scott and P. Bond, *Biochem. Soc. Trans.*, 2008, **36**, 27–32.
55 M. Parrinello and A. Rahman, *J. Appl. Phys.*, 1981, **52**, 7182–7190.
56 W. Deng and E. Barkai, *Phys. Rev. E*, 2009, **79**, 011112.
57 S. Burov, J.-H. Jeon, R. Metzler and E. Barkai, *Phys. Chem. Chem. Phys.*, 2011, **13**, 1800–1812.
58 J.-H. Jeon and R. Metzler, *Phys. Rev. E*, 2012, **85**, 021147.
59 Y. He, S. Burov, R. Metzler and E. Barkai, *Phys. Rev. Lett.*, 2008, **101**, 058101.
60 M. Patra, M. Karttunen, M. T. Hyvönen, E. Falck, P. Lindqvist and I. Vattulainen, *Biophys. J.*, 2003, **84**, 3636–3645.
61 M. Patra, M. Karttunen, M. T. Hyvönen, E. Falck and I. Vattulainen, *J. Phys. Chem. B*, 2004, **108**, 4485–4494.
62 V. Tejedor, O. Benichou, R. Voituriez, R. Jungmann, F. Simmel, C. Selhuber-Unkel, L. B. Oddershede and R. Metzler, *Biophys. J.*, 2010, **98**, 1364–1372.
63 M. Magdziarz, A. Weron, K. Burnecki and J. Klafter, *Phys. Rev. Lett.*, 2009, **103**, 180602.
64 B. A. Scalettar, J. R. Abney and J. C. Owicki, *Proc. Natl. Acad. Sci. U. S. A.*, 1988, **85**, 6726–6730.
65 D. F. Kusic, E. L. Elson and M. P. Sheetz, *Biophys. J.*, 1999, **76**, 314–322.
66 M. R. Horton, F. Hofling, J. O. Radler and T. Franosch, *Soft Matter*, 2010, **6**, 2648–2656.
67 K. A. Dill, K. Ghosh and J. D. Schmit, *Proc. Natl. Acad. Sci. U. S. A.*, 2011, **108**, 17876–17882.